International Journal of Applied Mathematics in Control Engineering 6 (2023) 110-116

Contents lists available at YXpublications

International Journal of Applied Mathematics in Control Engineering

Journal homepage: http://www.ijamce.com

Economic Scheduling Strategy for Microgrid Cluster in Multiple Scenarios Based on Improved Wild Dog Algorithm

Baoshan Qian, Zhaoxing Ma*, Jinxin Liu, Shuo Liu

School of Information and Control Engineering, Qingdao University of Technology, Qingdao Shandong, 266520, China

ARTICLE INFO

Article history:
Received 24 March 2023
Accepted 30 April 2023
Available online 8 May 2023

Keywords:
Microgrid cluster
Improved Wild Dog Algorithm
Economic dispatch
Latin hypercube sampling

ABSTRACT

Taking into account factors such as power generation cost, energy interaction cost, and environmental benefits of the microgrid cluster system, and considering the uncertainty of wind and solar power generation, an economic dispatch strategy for the microgrid cluster is constructed. Firstly, this article uses Latin hypercube sampling and scenario reduction methods to form typical scenarios for wind and photovoltaic power generation; Secondly, the Tent chaotic map and Gaussian mutation operator are used to improve the Dingo Optimization Algorithm, and the established objective function is solved by Improved Dingo Optimization Algorithm; Finally, simulation analysis was conducted on the scheduling strategy of the microgrid cluster, and the conclusion was drawn that the optimization scheduling analysis of the microgrid cluster system can improve the efficiency and economy of the microgrid cluster operation decision-making.

1. Introduction

At present, the world is facing issues such as the strengthening of the greenhouse effect and the shortage of fossil fuels. In order to promote ecological civilization construction and reduce energy waste, China has proposed the "dual carbon" target plan. In this context, the microgrid composed of distributed power generation devices such as wind power and photovoltaic, as well as energy storage and load, provides a good power network architecture for the development strategy of carbon peaking and carbon neutrality. The rapid development of microgrid technology has provided new technological ideas for the maturity of China's power supply technology, which not only effectively improves the utilization rate of renewable energy, but also improves the power supply efficiency in remote areas. Although microgrids provide users with a good and flexible platform for power supply, the inherent volatility and randomness of wind and photovoltaic power bring many challenges to the safe and stable operation of microgrids. The capacity of a single microgrid is limited. When the microgrid is greatly affected by the instability of distributed power generation devices during operation, a microgrid cluster composed of multiple interconnected microgrids can enhance the power supply reliability of the single microgrid and improve the grid's ability to resist interference. Therefore, under the requirements of the "dual carbon" target plan, it is particularly important to promote the optimized operation ability of micro grid clusters and improve their economy and reliability.

With the deepening of research on micro grid cluster interconnection technology by many scholars, certain research results have been achieved. Reference [5] constructs a distributed energy management system and proposes algorithms for efficiency compromise by endowing a single microgrid with power trading pricing power and trading power determination power with other microgrids. Reference [6] established a two-stage energy management model for micro grid clusters based on the SoS architecture to address the issue of unstable power supply caused by extreme weather conditions. This model maximizes power supply through the exchange of power generation resources between microgrids. Reference [7] aims to minimize voltage fluctuations and system losses in the microgrid cluster, and uses an improved multi-objective genetic algorithm and an AC DC hybrid power flow algorithm to solve the optimization model. Reference [8] established a dynamic economic scheduling model that takes into account the installation cost, operating cost, and environmental benefits of the microgrid cluster. The particle swarm optimization algorithm combined with Monte Carlo simulation was used to optimize the microgrid cluster, and the impact of different confidence levels on the optimization scheduling was analyzed. Reference [9] adopts a hierarchical peer-to-peer control strategy, treating a single microgrid in the microgrid cluster as an energy storage device, which solves the energy imbalance problem of the

* Corresponding author.
E-mail addresses: mazhaoxing@qut.edu.cn (Z. Ma)
doi:

microgrid cluster's sub-network and promotes the improvement of renewable energy utilization efficiency. Reference [10] takes into account the penetration rate of renewable energy while aiming to maximize the annual revenue of the microgrid cluster. Immune genetic algorithm is used to optimize the configuration of the microgrid cluster, and the maximum annual revenue of the microgrid cluster under high penetration rate is compared with the maximum annual revenue of the non-formed regional microgrid cluster system, proving that forming a microgrid cluster system can effectively improve the economic efficiency of power grid operation.

Based on the above research background, in order to achieve self-sufficiency and mutual assistance of individual microgrids within the microgrid cluster, this paper proposes an economic scheduling scheme for microgrid clusters in multiple scenarios based on an improved wild dog algorithm. In the day ahead scheduling phase, multi scenario generation technology is used to simulate the randomness of wind power and photovoltaic prediction of a single microgrid; In terms of functional models, an optimization scheduling model is constructed that takes into account the generation cost, energy interaction cost, and environmental benefits of the microgrid cluster system. By reasonably setting the energy storage capacity of each single microgrid, the adjust ability of renewable energy generation such as wind power and photovoltaic is improved; In terms of optimization algorithms, in order to improve the algorithm's traversal performance and ability to jump out of local optima during the initialization stage, Tent chaotic mapping and normal distribution operators are used to improve the Dingo Optimization Algorithm (DOA), and the Improved Dingo Optimization Algorithm (IDOA) is used to solve the optimization scheduling model, in order to achieve the lowest generation cost in the microgrid cluster system The purpose of minimizing the cost of electricity interaction and maximizing environmental benefits, and verifying the correctness and effectiveness of the proposed optimization strategy.

2. microgrid cluster system architecture

This article divides the microgrid cluster system into two levels: the first level is the main control center of the microgrid cluster, and the second level is the sub control center of each single microgrid. Each single microgrid is composed of Wind Turbines(WT), Photovoltaic Units(PV), Gas Turbines(GT), Battery(BAT) and loads. The system structure of the micro grid cluster is shown in Figure 1.

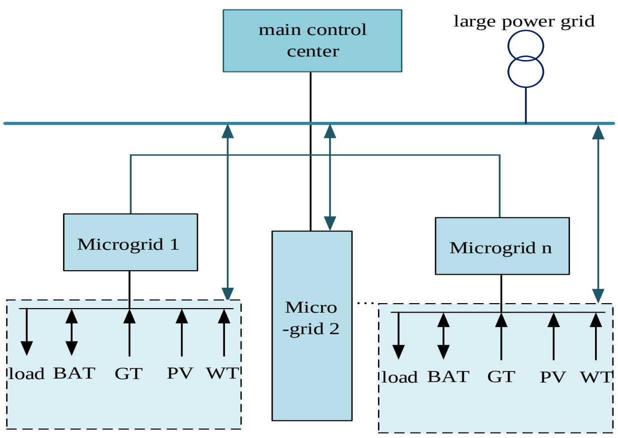

Fig. 1. microgrid cluster system structure diagram

The supply and demand requirements of each single microgrid during the same time period are different, and the scheduling requirements of the microgrid cluster system also vary. To ensure the coordinated operation between the single microgrid and the microgrid cluster, as well as between the microgrid cluster and the large power grid, this article adopts a hierarchical optimization approach to develop an optimized scheduling strategy for the microgrid cluster, which is detailed as follows:

(1) Optimal scheduling between microgrids and microgrid clusters

The microgrid transmits power generation information to the microgrid cluster control center through the regional microgrid sub control center. When the renewable energy generation capacity of each regional microgrid is sufficient, priority is given to charging the energy storage device before selling electricity to the microgrid cluster; When the renewable energy generation capacity of each microgrid is insufficient, arrange energy storage devices to supply power to the microgrid, with the goal of maximizing the economic benefits of the microgrid cluster, coordinate the output of each regional microgrid, and maximize the local consumption of each regional microgrid. At the same time, achieve coordination and cooperation between the microgrid and the microgrid cluster.

(2) Optimal scheduling between microgrid cluster and large power grid

The microgrid cluster control center analyzes the power generation information collected by the regional microgrid sub control center, and combines the electricity price situation at different time periods. When the renewable energy and energy storage generation capacity of the microgrid cluster are insufficient to support load demand, the cost of purchasing electricity from the large power grid and the cost of generating gas units are considered separately, with the goal of optimizing the overall economic benefits of the system, and achieving coordinated scheduling between the microgrid cluster and the large power grid.

3. Target model

3.1 Objective function

3.1.1 Operating costs

The operating costs include the cost of purchasing electricity from the large power grid, the cost of generating electricity from gas turbines, the cost of operating energy storage equipment, and the cost of abandoning wind and solar energy.

$$F_1 = F_{i,t}^{\mathrm{grid}} + F_{i,t}^{GT} + F_{i,t}^{BAT} + F_{i,t}^{loss} \tag{1}$$

In the formula, $F_{i,t}^{grid}$ is the cost of purchasing electricity from the large power grid in the period t for the ith microgrid, $F_{i,t}^{GT}$ is the cost of generating electricity from the gas turbine in the period t for the ith microgrid, $F_{i,t}^{\mathrm{BAT}}$ is the operating cost of energy storage equipment in the period t for the ith microgrid, and $F_{i,t}^{loss}$ is the cost of abandoning wind power and Photovoltaic power in the period t for the ith microgrid. The cost of purchasing electricity from large power grid can be expressed as:

$$F_{i,t}^{grid} = \sum_{i=1}^{N}\sum_{t=1}^{T} R_{i,t} P_{i,t}^{grid} \tag{2}$$

In the formula, N is the number of microgrids, T is the number of time periods during the scheduling period, $R_{i,t}$ and $P_{i,t}^{grid}$ are the electricity prices and power purchased from the large power grid in the period t for the ith microgrid.

The cost of Gas Turbine power generation can be expressed as:

$$F_{i,t}^{GT}=\sum_{i=1}^{N}\sum_{t=1}^{T}\left[aP_{i,t}^{GT^2}+bP_{i,t}^{GT}+c\right] \quad (3)$$

In the formula, $P_{i,t}^{GT}$ is the power generated by the gas turbine in the period t for the ith microgrid, a, b, and c are the cost coefficients of the gas turbine fuel.

The operating cost of energy storage equipment can be expressed as:

$$F_{i,t}^{BAT}=\sum_{i=1}^{N}\sum_{t=1}^{T}R_{i,t}^{BAT}\left(-\frac{P_{i,t}^{BAT^c}}{\gamma}+\gamma P_{i,t}^{BAT^d}\right) \quad (4)$$

In the formula, $R_{i,t}^{BAT}$ is the operating cost coefficient of the energy storage equipment in the period t for the ith microgrid, γ is the charging and discharging efficiency of the energy storage, $P_{i,t}^{BAT^c}$ and $P_{i,t}^{BAT^d}$ is the charging and discharging power of the energy storage in the period t for the ith microgrid.

The cost of abandoning wind power and Photovoltaic power can be expressed as:

$$F_{i,t}^{\text{loss}}=\sum_{i=1}^{N}\sum_{t=1}^{T}R_{i,t}^{loss}P_{i,t}^{loss} \quad (5)$$

In the formula, $R_{i,t}^{loss}$ is the cost coefficient of wind power and Photovoltaic power abandonment in the period t for the ith microgrid, and $P_{i,t}^{loss}$ is the amount of wind power and Photovoltaic power abandonment in the period t for the ith microgrid.

3.1.2 Energy interaction cost

$$F_2=\sum_{i=1}^{N}\sum_{t=1}^{T}R'_{i,t,i+1}P'_{i,t,i+1} \quad (6)$$

In the formula, F_2 is the cost of electricity interaction between the ith microgrid and other microgrids in the period t, $R'_{i,t,t+1}$ and $P'_{i,t,i+1}$ is the cost coefficient and power of the energy interaction between the ith microgrid and the ith+1 microgrid in the period t.

3.1.3 Environmental benefit

$$F_3=\sum_{i=1}^{N}\sum_{t=1}^{T}\sum_{m=1}^{M}(P_{i,t}^{\text{BAT}}+P_{i,t}^{GT})\ \gamma_{i,m}(t)s_{i,m} \quad (7)$$

In the formula, F_3 is the cost of environmental pollution control; M is the type of pollutant (M=5, representing CO_2, CO, SO_2, $PM_{2.5}$, NO_X), $\gamma_{i,M}(t)$ is the emission coefficient of the mth pollutant generated by the ith microgrid in the period t; $S_{i,m}$ is the cost coefficient of the mth pollutant generated by the ith microgrid in the period t.

3.2 Constraint condition

(1) Power balance constraints

$$P_{i,t}^{PV}+P_{i,t}^{WT}+P_{i,t}^{BAT}+P_{i,t}^{GT}+P_{i,t}^{grid}+P_{i,t}^{loss}-P_{\text{load,t}}=0 \quad (8)$$

(2) Power generation constraints

$$P_{\min}^{j}\le P_{i,t}^{j}\le P_{\max}^{j} \quad (9)$$

In the formula, $P_{i,t}^{j}$ is the generation power of the jth power source t period in the ith microgrid, $P_{\max}^{j}$ and $P_{\min}^{j}$ are the upper and lower limits of the generation power of the jth power source, respectively. j can be represented as a set as j={PV, WT, grid, BAT, GT}.

(3) Capacity constraints of energy storage equipment

$$C_{i,t,\min}^{BAT}\le C_{i,t}^{BAT}<C_{i,t,\max}^{BAT} \quad (10)$$

In the formula, $C_{i,t}^{BAT}$ is the capacity of the energy storage device bat, $C_{i,t,\min}^{BAT}$ and $C_{i,t,\max}^{BAT}$ are the maximum and minimum values of the bat energy storage capacity, respectively.

Taking into account the operating costs, energy interaction costs, and environmental benefits of the microgrid cluster, the optimal objective function for the economic benefits of the microgrid cluster is as follows:

$$\min F=F_1+F_2+F_3 \quad (11)$$

4. Optimization algorithm

4.1 Dingo Optimization Algorithm

This article uses IDOA to solve the established objective function to achieve the optimal economic benefits. This algorithm was proposed by Herna´n Peraza-Va´zquez et al. in 2021 [11], and simulates four strategies of wild dogs during predation. These four strategies are siege, pursuit, decay, and survival. Among them, siege, pursuit, and decay are mutually exclusive strategies, and each wild dog chooses one of these three strategies for optimization, After going through the survival strategy, a new location is finally obtained. The specific algorithm introduction and optimization process have been detailed in literature [12], and this article will not elaborate further. The following will focus on the improvement of this algorithm in this article.

4.2 Improved Dingo Optimization Algorithm

Although DOA has the characteristics of fast convergence speed and strong local search ability, but the algorithm has a slow search speed in the early stage and insufficient ability to jump out of local optima in the later stage. In response to these problems, the present invention introduces tent chaotic mapping in the initialization stage of the DOA algorithm and Gaussian mutation operator in the survival strategy stage. The specific improvement methods are as follows:

(1) To enhance the early convergence speed of the algorithm, the present invention adopts a tent chaotic map that can improve the population diversity in the search space to improve the initialization stage of the algorithm. The expression of the tent chaotic map is as follows:

$$l_{n+1}=\begin{cases} l_n/\alpha, l_n\in[o,\alpha) \\ (1-l_n)/(1-\alpha), l_n\in[\alpha,1) \end{cases} \quad (12)$$

In the formula, $l_n\in[0,1]$ is the function value of the chaotic map; α is system parameters within the range of (0,1).

At this point, the update formula for the initialization phase is:

$$X_i=l_n(ub_i-lb_i)+lb_i \quad (13)$$

(2) To improve the ability of the algorithm to jump out of local optima in the later stage, the present invention introduces a Gaussian mutation operator that can improve the activity of the algorithm population, and the expressions are as follows:

$$f(x) = \frac{e^{-\left(\frac{x^2}{2}\right)}}{\sqrt{2\pi}} \tag{14}$$

After introducing the Gaussian mutation operator, the update formula for the survival strategy is as follows:

$$X'_{new,i} = X_{new,i} + X_{new,i} \cdot f(x) \tag{15}$$

The IDOA algorithm, which introduces Gaussian mutation operator, has a strong ability to jump out of local optima. By using the IDOA algorithm to solve the objective function, the economic benefits of microgrid cluster optimization scheduling can be maximized.

4.3 IDOA algorithm solving process

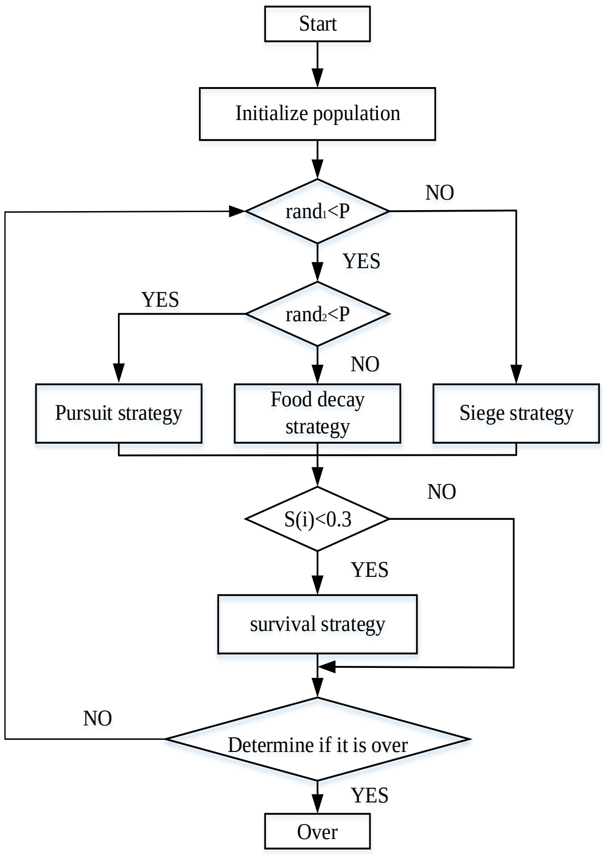

Fig. 2. Solution flow of IDOA algorithm

5. Example analysis

The uncertainty of renewable energy output such as wind power and photovoltaic power poses great challenges to microgrid cluster systems. Therefore, this article constructs a multi scenario power generation prediction for typical wind and photovoltaic power, and selects scenarios 1, 2, and 3 from the generated typical wind and photovoltaic power generation scenarios as the wind and photovoltaic power output predictions for each single microgrid in the microgrid cluster system studied in this article.

5.1 Multi scenario construction of wind and photovoltaic power generation

This article takes into account the randomness of wind power and photovoltaic power, and uses multi scenario generation technology to model and analyze wind power and photovoltaic power. The model is as follows:

$$P_{j,t,s}^{typ} = P_{j,t}^{hist}\left(1 + \xi_j R_{j,t} - \xi_j \delta\right) \tag{16}$$

In the formula, $P_{j,t,s}^{typ}$ is the predicted power value of typical daily scenario s during time period *t*; $P_{j,t}^{hist}$ is the predicted daily power of time period *t* obtained from historical numerical predictions; ξ_j is the percentage of prediction error threshold; $R_{j,t}$ is a random number; δ is the correction factor for random distribution; The subscript *j* refers to wind turbines and photovoltaic units.

In general, the prediction error of photovoltaic power follows a normal distribution, while the prediction error of wind power follows a Beta distribution representation [13]. The probability distribution is as follows:

$$f(R_{j,t}) = \frac{1}{\sigma\sqrt{2\pi}} e^{-\frac{(R_{j,t}-\mu)^2}{2\sigma^2}} \tag{17}$$

$$f(R_{j,t}) = N_d R_{j,t}^{\alpha-1}\left(1 - R_{j,t}\right)^{\beta-1} \tag{18}$$

In the formula, μ and σ expectations and variances of normal distributions, respectively; α and β The shape and scale parameters of the Beta distribution, respectively; N_d is the normalization factor.

On the basis of the above prediction model, this article uses Latin hypercube sampling technology to generate multiple scenarios [14]. The main steps are:

(1) Solve the value x_i within any interval $[x_1,x_n]$ and obtain the probability distribution function value of $f(x_i)$, From this, the interval $[f(x_1),f(x_n)]$ on the vertical axis of the probability distribution function graph can be obtained, and the probability distribution can be equally divided into n probability intervals.

(2) Sample the n divided probability intervals and use the random number P_i within the interval as the sampling points.

(3) Perform inverse transformation on probability distribution function $f(x_i) = P_i$ to obtain sample value x_i at sampling point.

Generating a large number of scenarios can increase the difficulty of solving. To reduce the difficulty of solving, this article uses synchronous back-stepping method to reduce the sample scenarios. The reduced typical scenarios can also reflect the probability distribution of wind and photovoltaic power. The scenario reduction process based on synchronous back-stepping method is as follows [15]:

(1) Calculate any scene x_i and the scene x_j closest to it.

$$D_i = \min \theta_i d(x_i, x_j),\ j = 1,2,\cdots,N,\ \ j \neq i \tag{19}$$

In the formula, D_i is the probability distance from scene x_i; θ_i is the probability of scenario x_i; $d(x_i, x_j)$ is the Euclidean distance between scene x_i and x_j.

(2) Identify the scenes that need to be deleted x_i.

$$D_{\min} = \min \theta_i D_i,\ i = 1,2,\cdots,N \tag{20}$$

In the formula, $D_{\min}$ is the probability distance closest to scene x_i.

(3) Delete the determined scenario x_i above and add the probability of deleting the scenario to the probability of the nearest sample x_j, ensuring that the sum of probabilities is 1. Repeat the above steps until the remaining number of scenes reaches the set

value. After generating and reducing the above scenes, the typical number of wind power and photovoltaic scenes are finally obtained as N_{WT} and N_{PV}, respectively. Finally, the number of typical scenario combinations N_s and the corresponding probability of typical scenario combinations are:

$$N_s = N_{WT} N_{PV} \tag{21}$$

$$\theta_s = \theta_{WT} \theta_{PV}, s = 1,2,\cdots N_S \tag{22}$$

In the formula, θ_{WT} and θ_{PV} represents the probability corresponding to wind and photovoltaic power scenarios.

This article generates intraday random scenarios based on Latin hypercube sampling technology, μ and σ take 0.47 and 0.31 respectively, α and β take 2.35 and 0.5 respectively, the relative errors for photovoltaic and wind power are 20% and 30%, respectively. After using the synchronous back-stepping method to reduce the daily random scenes, the number of typical scenes for photovoltaic and wind power is 5. The typical scenes for wind power during the day are shown in Figure 3, and the typical scenes for photovoltaic power during the day are shown in Figure 4.

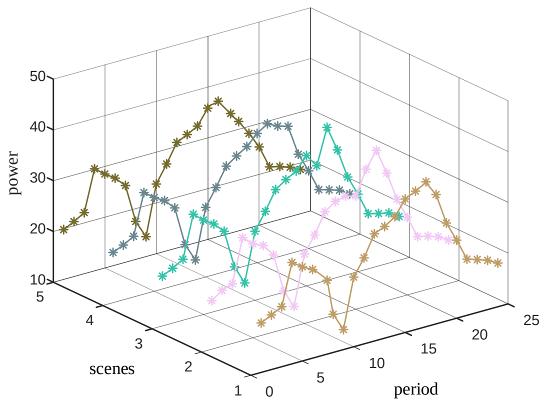

Fig. 3. Typical scenario of wind power during the day

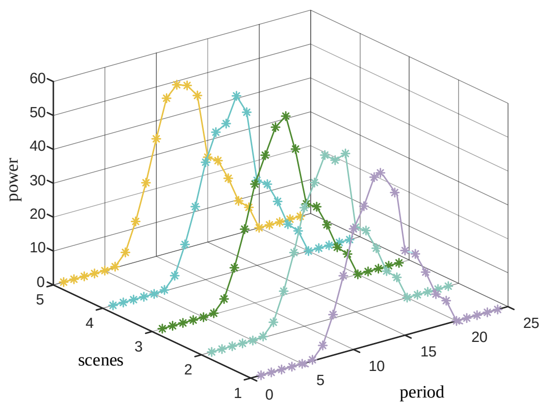

Fig. 4. Typical Photovoltaic Day Scenarios

5.2 Example Introduction

The micro grid cluster system established in this article is composed of three single microgrids, and the predicted wind and photovoltaic output of these three single microgrids is selected from scenarios 1, 2, and 3 generated by the scene generation method. Each micro grid includes four distributed power sources: photovoltaic units, wind turbine units, micro gas turbines, and batteries. This article sets a typical day divided into 24 time periods for optimized scheduling. The time of use electricity price is set according to the current electricity price, with a valley period electricity price of 0.16 yuan/kWh, a regular period electricity price of 0.45 yuan/kWh, and a peak period electricity price of 0.79 yuan/kWh. The parameters of each micro power supply in the multi microgrid system are shown in Table 1 [16], and the pollutant emission coefficients of each micro power supply are shown in Table 2 [17]-[18]:

Tab. 1. Parameters of each micro power supply

parameter	Fuel cost (yuan/kWh)	Power interaction cost(yuan/kW)	Lower limit of output/kW	Upper limit of output/kW
PV1	0	0.0096	0	60
WT1	0	0.03	0	50
CGS1	0.211	0.128	0	30
BAT1	0	0.035	-30	30
PV2	0	0.0096	0	60
WT2	0	0.03	0	50
CGS2	0.211	0.128	0	30
BAT2	0	0.035	-40	40
PV3	0	0.0096	0	60
WT3	0	0.03	0	50
CGS3	0.211	0.128	0	30
BAT3	0	0.035	-50	50
Grid	0	0	-100	100

Tab. 2. pollutant emission coefficient of each micro power supply

Types of pollutants	Pollutant emission coefficient(g/kWh)		Pollutant treatment fee (yuan/kg)
	BAT	GT	
CO2	649	724	0.21
CO	0	0.047	10.29
SO2	0.206	0.0036	14.842
PM2.5	0	0	30.55
NOX	0.08	0.2	62.964

5.3 scheduling strategy

Strategy 1: On the premise that energy storage devices participate in economic dispatch, wind and photovoltaic power are prioritized to supply power to the microgrid. If the microgrid load demand is met, energy storage devices are arranged for charging. If the microgrid load demand is not met, electricity is purchased from the large power grid.

Strategy 2: Based on the participation of energy storage devices in economic dispatch, it is arranged that power can be freely exchanged between micro grids. When the cost of purchasing power from micro grid to wind power and photovoltaic power is higher than that from large grid, the large grid has priority to transmit power to micro grid. If the cost of purchasing power from wind power and photovoltaic power is lower than that from large grid, the microgrid is arranged to sell the remaining power to large grid to obtain higher economic benefits.

The total cost of microgrid cluster power generation for the two scheduling strategies selected in this article is shown in Table 3:

Tab. 3. Optimization Results under Different Optimization Strategies

Strategy	1/yuan	2/yuan
total cost	1678	1531

From Table 3, it can be seen that making reasonable planning for the power scheduling strategy of microgrid cluster can significantly reduce the total power generation cost of microgrid cluster, reflecting the feasibility of the optimization strategy proposed in this article.

Under the above scheduling strategy, the micro power output of each microgrid is shown in Figures 5, 6 and 7 respectively.

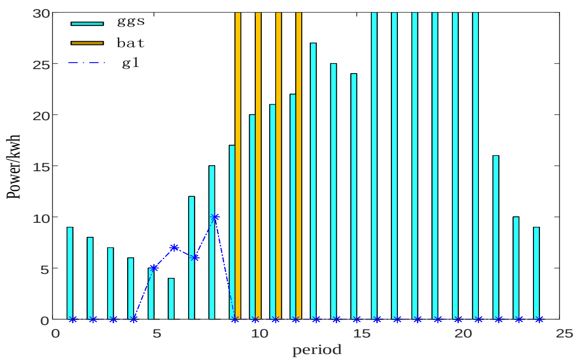

Fig. 5. power output of microgrid 1

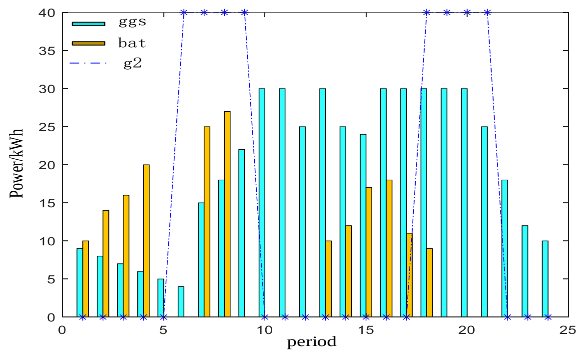

Fig. 6. power output of microgrid 2

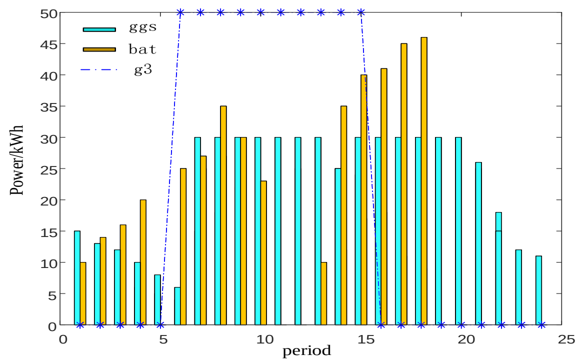

Fig. 7. Output of Each Power Supply in microgrid 3

As shown in Figures 5-7, the electrical energy between each microgrid is freely coordinated and mutually beneficial, and the microgrid cluster system aims to achieve the optimal economic benefits and achieve coordinated scheduling of microgrid cluster electrical energy. From Figure 5, it can be seen that the cost of purchasing electricity from the large power grid from 5:00 to 8:00 is relatively low. From 9:00 to 12:00, the remaining electricity generated by the microgrid is transmitted to microgrid 2 and microgrid 3; From Figure 6, it can be seen that microgrid 2 purchases a large amount of electricity from the large power grid from 5:00 to 10:00 and 18:00 to 21:00. During the time period from 22:00 to 24:00, microgrid 2 has sufficient electricity and does not need to purchase electricity from the large power grid; From the output of each power source in microgrid 3 in Figure 7, it can be seen that there is a significant power gap in microgrid 3, and it is necessary for microgrid 1 and microgrid 3 to supplement the power gap.

The results of microgrid cluster coordination and mutual aid optimization are shown in Figure 8:

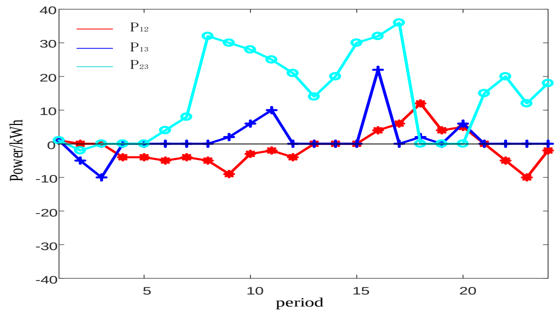

Fig. 8. Coordination and Mutual Aid Optimization Results of Micro grid Cluster

As shown in Figure 8, P_{12} and P_{13} represent the electrical energy transmitted from microgrid 1 to microgrid 2 and microgrid 3, respectively, while P_{23} represents the electrical energy transmitted from microgrid 2 to microgrid 3. During the periods of 3:00-13:00 and 21:00-24:00, the distributed power output of microgrid 1 is insufficient to maintain the load demand of microgrid 1. During this period, microgrid 2 transmits electricity to microgrid 1, and during the period of 15:00-21:00, microgrid 1 transmits electricity to microgrid 2 and microgrid 3; The output of microgrid 2 during the periods of 5:00-18:00 and 20:00-24:00 meets its own needs while transmitting electricity to microgrid 3; microgrid 3 has sufficient distributed power output between 1:00 and 4:00, transmitting surplus electricity to microgrid 1 and microgrid 2. Each microgrid coordinates and transfers surplus electricity to each other through interactive strategies.

6. Conclusion

On the basis of considering the uncertainty of wind and photovoltaic power generation, this article uses Latin hypercube sampling and scenario reduction method to generate typical wind and photovoltaic power generation scenarios, in order to simulate the randomness of microgrid wind and photovoltaic prediction, and proposes a set of optimization strategies for microgrid cluster economic adjustment. Finally, through numerical analysis, it is shown that allowing microgrid clusters to freely transmit electricity to the large grid can improve the economy of the microgrid, reduce energy losses, and reduce the power supply pressure of the large grid. The optimization scheduling analysis of the microgrid cluster system can improve the efficiency and economy of the operation decision-making of the microgrid cluster.

Acknowledgements

This work is Supported by the National Natural Science Foundation of China (62203248), Shandong Natural Science Foundation General Support Project (ZR2020ME194, ZR2021MF087).

References

[1] Shu Y B, Zhang L Y, Zhang Y Z, et al. Carbon Peak and Carbon Neutrality Path for China’s Power Industry[J]. Strategic Study of CAE, 2021, 23(6): 1-14.

[2] Chen S, Wei Z N, Gu W, et al. Carbon neutral oriented transition and revolution of energy systems：multi-energy flow coordination technology[J]. Electric Power Automation Equipment, 2021, 41(9): 3-12.

[3] SOLANKI B V, RAGHURAJAN A, BHATTACHARYA K, et al. Including smart loads for optimal demand response in integrated energy management systems for isolated microgrids[J]. IEEE Transactions on Smart Grid, 2017, 8(4): 1739-1748.

[4] Lu T G, Ai Q, Sun S M, et al. Behavioural analysis and optimal operation of active distribution system with multi-microgrids[J]. Proceedings of the CSEE, 2016, 36(1): 122-132(in Chinese).

[5] Li D M, Wu Z J, Zhao B. Cooperative game model and optimal dispatch strategy of multi-microgrid system[J/OL]. Proceedings of the CSEE, 2022, 42(14): 14-5140-14.

[6] Chen Z J, Chen M Y, Zhao B, er al. Resilience enhancement strategies for extreme scenarios of multi-microgrid based on system of systems architecture[J]. Automation of Electric Power Systems, 2021, 45(22): 29-37(in Chinese).

[7] Zhang S Z, Pei w, Yang Y H, et al. Optimization and analysis of multi-microgrids integration and aggregation operation based on flexible DC interconnection[J]. Transactions of China Electrotechnical Society, 2019, 34(5): 1025-1037.

[8] Wu H B, Sun R S, Cai G Y. Dynamic economic dispatch for multi-microgrid interconnection system[J]. Acta Energiae Solaris Sinica, 2018, 39(5): 1426-1433.

[9] Wang Y H, Li Z J, Hou M, et al. Research on hierarchical peer-to-peer control and power management strategies for DC microgrid clusters[J]. Renewable Energy Resources, 2023, 41(03): 385-393.

[10] Wang S X, Zhang Q, Wang H, et al. Optimal planning method for regional multi-microgrid system with high renewable energy penetration[J]. Electric Power Automation Equipment, 2018, 38(12): 33-52.

[11] Cai X L, Zhu J Z, Liu M, et al. Peak shaving strategy of electric vehicles based on an improved Dingo optimization algorithm[J]. Energy Storage Science and Technology, 2023, 12(6): 1913-1919.

[12] Sun H R, Li J, Dong Z. Model Identification of SCR Denitration System Based on Quantum Behavior and Lévy Flight Improved Dingo Algorithm[J].Shandong Electric Power, 2023, 50(06): 44-51.

[13] Li Y, Yang Z, Li G. Optimal scheduling of an isolated microgrid with battery storage considering load and renewable generation uncertainties[J]. IEEE Transactions on Industrial Electronics, 2019, 66(2): 1565-1575.

[14] Han Z Y, Zhang Y H, Li B. Two-stage optimal dispatching of CCHP virtual power plant based on multi-scenario technology[J]. Electrical Measurement ＆ Instrumentation, 2022, 59(3): 174-180.

[15] Wei B, Han X Q, Li W, et al. Multi-time Scale Stochastic Optimal Dispatch for AC/DC Hybrid Microgrid Incorporating Multi-scenario Analysis[J]. High Voltage Engineering, 2020, 46(7): 2359-2369.

[16] Xiao H, Pei W, Kong L. Multi-time scale coordinated optimal dispatch of microgrid based on model predictive control[J]. Automation of Electric Power Systems, 2016, 40(18): 7-14, 55.

[17] Wu M, Luo Z, Ji Y. Optimal dynamic dispatch for combined cooling heating and power microgrid based on model predictive control[J]. Proceedings of the CSEE, 2017, 37(24): 7174-7184+7431.

[18] Meng A B, Lin Y C, Yin H. Synergetic scheduling optimization method of grid-connected home wind-solar-storage system considering uncertainty factors[J]. Power System Technology, 2018, 42(1): 162-173.

Baoshan Qian is currently pursuing a master's degree in Information and Engineering at Qingdao University of Technology. She obtained a bachelor's degree from Yancheng Teachers University in 2020. Her main research direction is the coordinated optimization problem of source network load storage in new power systems.
Email: Q18036285933@126.com

Zhaoxing Ma is currently a lecturer at Qingdao University of Technology. He obtained a Master's degree in Applied Mathematics from Harbin University of Science and Technology in 2009 and a PhD in Electrical Engineering from Southeast University in 2013. His main research direction is power system analysis, operation, and comprehensive energy system planning.
Email: mazhaoxingapple@126.com

Jinxin Liu is currently pursuing a master's degree at Qingdao University of Technology in Qingdao, China. He received his Bachelor of Engineering degree from Weifang University of Science and Technology in 2021, and his main research direction is the research of multi-user load forecasting technology under new power systems.
Email: l159357dd@163.com

Shuo Liu is currently pursuing a master's degree in Information and Control Engineering at Qingdao University of Technology. He obtained a Bachelor's degree in Engineering from Yantai Nanshan University in 2022, and his main research direction is the study of multi-level coordinated dispatch strategies for new power systems.
Email: 1269416091@qq.com